PERIODICO di MINERALOGIA
established in 1930

Dipartimento di Scienze della Terra
Sapienza Università di Roma

An International Journal of
Mineralogy, Crystallography, Geochemistry,
Ore Deposits, Petrology, Volcanology
and applied topics on Environment, Archaeometry and Cultural Heritage

Characterization of recently discovered common green opals from Anosy (Madagascar)

Franca Caucia *, Luigi Marinoni, Mattia Gilio, Eleonora Dal Corso

Department of Earth and Environmental Sciences, University of Pavia, Via Ferrata 1, 27100 Pavia, Italy

ARTICLE INFO

Submitted: August 2020
Accepted: November 2020
Available on line: January 2021

* Corresponding author:
caucia@crystal.unipv.it

Doi: 10.13133/2239-1002/16982

How to cite this article:
Caucia F. et al. (2021)
Period. Mineral. 90, 217-228

ABSTRACT

The recently discovered common green opals from Anosy in Madagascar were studied for their physical, chemical and gemological properties and gemological relevance. The color of the opals is yellowish green but not very homogeneous for the presence of cavities, dark lamellae and spots, the diaphaneity is translucent / opaque with greasy luster and are inert to long and short wavelength UV radiation (366–254 nm). Refractive index and specific gravity values range between 1.435–1.460 and 2.03-2.07, respectively. The opals are CT type with tridymite more abundant than cristobalite and contain clay minerals (saponite). The main chromophores that determine the color are Fe and, subordinately, V and Cu. Other detected trace elements are Mg, Al, Ca, K, Na, Ni and Cr. The high contents of Ba, probably deriving from mica and feldspars, are noteworthy and can represent a geochemical marker. Three types of microstructures were observed: homogeneous and very fine microspheres, lepispheric cauliflower structures and globular aggregates of different sizes formed by laminae. Our analyses suggest that opals formed under similar genetic conditions, with a slow or moderate growth rate. Anosy opals would certainly have a good commercial value as semi-precious materials, although lower than those from other regions of Madagascar (Bemia).

Keywords: Opal, Madagascar; Geochemistry; SEM; Raman Spectroscopy; XRPD.

INTRODUCTION

Opals with the pleasant play of color effect are the most precious and have been the subject of uncountable researches. In contrast opals without this effect, also referred to as "common" opals, have been much less studied although may exhibit several beautiful colors and still have significant commercial value (Sanders, 1964; Eckert, 1998; Caucia et al., 2012a). Common opals have been mined worldwide: green opals from Peru, Tanzania and Turkey (Koivula and Fryer, 1984; Bank et al., 1997; Esenli et al., 2001; Brajkovic et al., 2007; Caucia et al., 2016; Hatipoglu and Yardimici, 2014; Hatipoglu et al., 2015), blue opals from Brazil and Peru (Brajkovic et al., 2007; Caucia et al., 2008, 2009; Ghisoli, 2008; Ghisoli et al., 2010; Koivula and Kammerling, 1991; Caucia et al. 2015) and purple opals from Turkey (Hatipoglu et al., 2015).

Madagascar is the world's leading producer of several gems such as ruby, sapphire, tourmaline, emerald, amethyst, aquamarine, garnet and also has some important opal deposits such as that of Faratsiho, located near the capital Antananarivo at the center of the island (Lacroix, 1922) and that near to the town of Bemia in the southeast corner of the island (Simoni et al., 2010).

For this work, the mineralogical, physical, gemological and geochemical properties of several samples of common green opal from the region of Anosy in Madagascar, not yet studied, have been investigated to evaluate their gemological relevance, to identify the chromophores responsible for color, to investigate the genetic conditions

and to compare with the characteristics of other opals from other regions of Madagascar and around the world.

GEOLOGICAL SETTING

Madagascar is a large island, off the southern coast of Africa, about 1600 km long from north to south and 600 km wide at its widest point. The lithologies that outcrop in most of the eastern part of Madagascar are mainly represented by very deformed metamorphic rocks spanning an age between Archean and Neoproterozoic (Ashwal and Tucker, 1999; Brandt et al., 2014; Moine and Nedelec, 2014). Differently the western part is covered by sub-horizontal sediments deposited over a period between the Carboniferous and the present.

The southern part of Madagascar underwent two different phases of high pressure deformation and metamorphism: the first phase took place at 620-600 Ma and affected the Androy and Vohibory domains while the second at 580-520 Ma and concerned the Androy and Anosy domains.

The Vohibory domain, located to the western side, is made of mafic and felsic igneous rocks with intercalations of paragneiss and vast layers of marble. Mafic rocks are believed to be basalts from the mid-ocean and island arc and their extrusion took place around ~850-700 Ma. Furthermore, the Vohibory domain was affected by the metamorphism of the East African orogen about 650-630 Ma.

Conversely, the Anosy-Androy domain is composed up by metasediments and mafic metavulcanites that correspond to the "southern granulite". The western margin includes the Anpanihy strain zone and the outcropping rocks are mainly paragneiss, ortogneiss, olivine-bearing gabbro, peridotite and alkaline granite (Ashwal and Tucker, 1999; Brandt et al., 2014).

The opals analyzed in this work derive from the south-eastern area of the island and belong to the Anosy-Androy geological domain.

MATERIALS AND METHODS

The samples investigated in this work were provided by a collector who purchased them from the deposit of Anosy. The opals were extracted from centimeter-sized rough samples selected on the base of the color tone (Figure 1) and were subsequently fashioned into cabochon gemstones. The sample size was measured using a Powerfix electronic digital caliper. None of the samples had sufficient adhering host rock allowing assessment.

The gemcut stones (Figure 2) were examined by standard gemological methods to determine refractive index, macroscopic color, optical properties, hydrostatic SG specific gravity/density, UV fluorescence (366-245 nm) and microscopic features.

Refractive index was determined with a Kruss Refractometer ER6040 using plain white light with a sodium filter (589 nm) and a methylene iodide as contact liquid (n=1.80), with a measurement range of n=1.30-1.80.

The color of the opal samples was assessed using the GIA gemstone color system to establish hue, tone and saturation scales. Hue is the first impression of the

Figure 1. Raw samples of the green opals from Anosy in Madagascar investigated in this paper; the dimensions of the samples (cm) are the following: sample: a: 2.3×2.2×7.1; sample b: 3.6×4.8×14.75; sample c: 2.1×2.4×7.8; sample d: 3.9×5.2×9.50; sample e: 1.9×2.4×3.9; sample f: 1.8×2.3×6.5; sample g: 1.7×2.4×6.1.

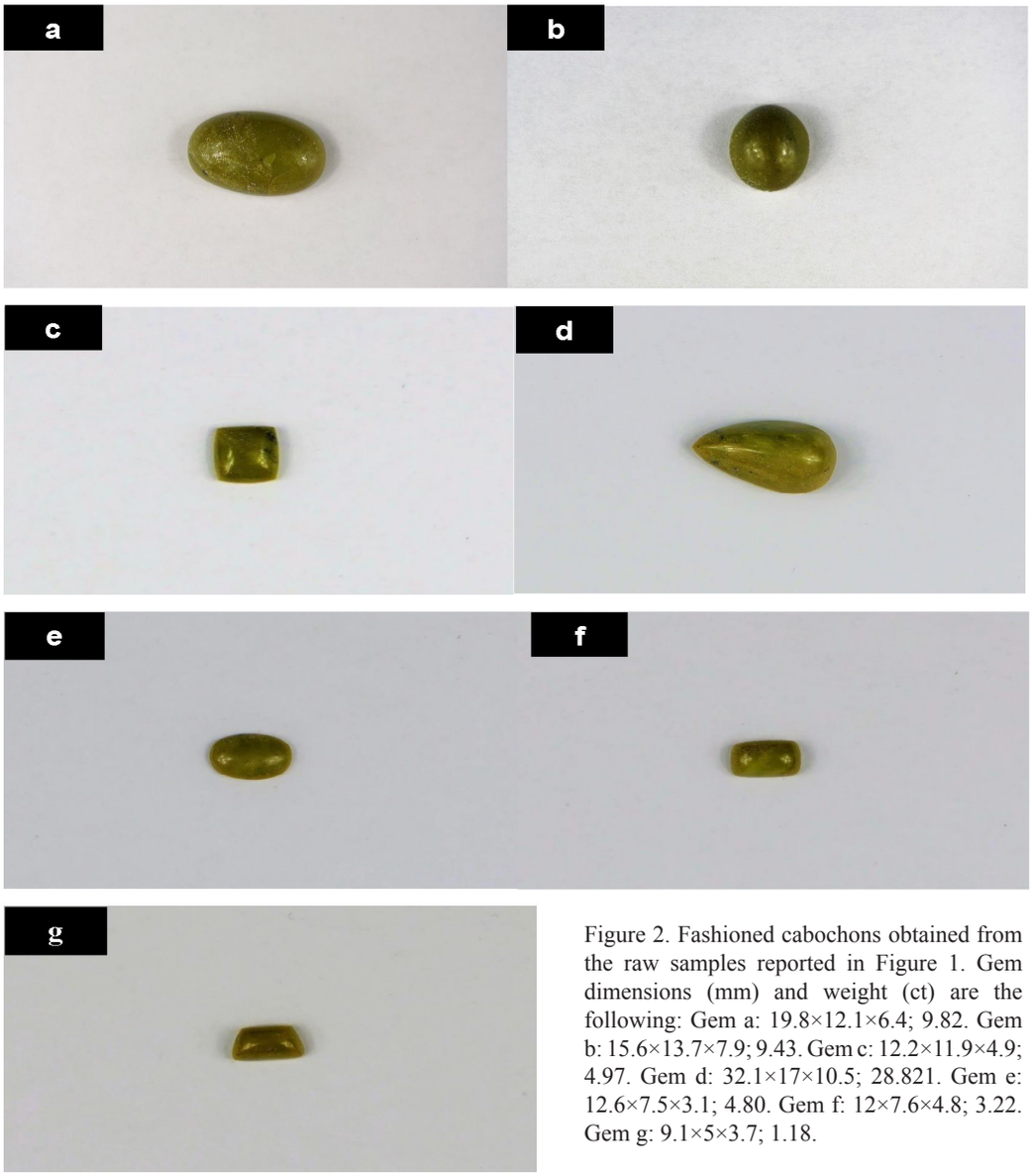

Figure 2. Fashioned cabochons obtained from the raw samples reported in Figure 1. Gem dimensions (mm) and weight (ct) are the following: Gem a: 19.8×12.1×6.4; 9.82. Gem b: 15.6×13.7×7.9; 9.43. Gem c: 12.2×11.9×4.9; 4.97. Gem d: 32.1×17×10.5; 28.821. Gem e: 12.6×7.5×3.1; 4.80. Gem f: 12×7.6×4.8; 3.22. Gem g: 9.1×5×3.7; 1.18.

basic color of an object (31 hues in the GIA scale: red, orange, yellow, green, blue, violet and the combination of these colors); tone is the degree of darkness or lightness of a color (11 levels GIA); saturation is the strength or intensity of a color (6 levels GIA). For reference, color was also graded using the Munsell Soil Book (Munsell 1912). Fluorescence of the opal samples in longwave (LW: 365 nm) and shortwave (SW: 254 nm) ultra-violet (UV) light was measured with a 4W EL Series UVLS-24 lamp from Analytik Jena.

Specific gravity was determined using a Presidium PC100 electronic scale with 0.005 of accuracy, and a glass pycnometer with distilled water at 25 °C as immersion fluid.

Microtexture and morphology of the opal samples was studied in a Zeiss Evo 40 MA10 scanning electron microscope (SEM) equipped with an Oxford Instruments Energy-dispersive spectrometer (EDS), using an electron beam at 20 kV and 500 pA, and nominal beam diameter set to 1μm. For the analyses, millimeter-sized fragments of untreated rough opal were mounted on aluminum stubs with double-sided carbon adhesive, and then coated with ~20 nm carbon in an Agar device to minimize charging under the ebeam.

X-ray Powder Diffraction (XRPD) data were collected at the Earth and Environmental Sciences Department with a Philips PW1800 powder diffractometer with Bragg-Brentano geometry and an automatic divergence slit,

CuKα radiation (λ=1.5418Å, 50 kV, 30 mA) and a scan speed of 1°/min, in the angular range between 2-65° 2θ (see Figure 3 a,b). The opal samples were firstly ground using an agata steel percussion mortar until they reduced to very fine powder and then mounted on the sample holder (see Moore and Reynolds, 1997). Qualitative and semi-quantitative analyses of the mineral phases in the opals have been valuated through the program "PANnalytical XPert HighScore" with an analytical error of about 5%. The tridymite versus cristobalite ratio was calculated by comparing the position of the characteristic peak in the interval *d*=4.04-4.11 Å whose extremes correspond respectively to the values of pure cristobalite and pure tridymite. CT opals show a peak corresponding to a d-value ranging from 4.06 to 4.11. For the evaluation of the two different components we used the following equation (Fritsch et al., 2004; Ghisoli et al., 2010):

$$C/T_{XRPD} = \frac{dTrd - dmeasured}{dTrd - dCrs} = \frac{4.11 - x\ Å}{4.11 - 4.04Å}$$

Micro-Raman scattering measurements were conducted at the Earth and Environmental Sciences Department with a Horiba Jobin-Yvon Explora Plus single monochromator spectrometer (with a grating of 2400 groove/mm) mounted on an Olympus BX41 microscope. Measurements were directly performed on the cabochon gems. Raman spectra were excited by the 532 nm line of an Ar laser. The spectrometer was calibrated to the silicon Raman peak at 520.5 cm^{-1}. The spectral resolution was ~2 cm^{-1} and the instrumental accuracy in determining the peak positions was ~0.56 cm^{-1}. Raman spectra were collected in the spectral range 50-1250 cm^{-1} and 3000-3800 cm^{-1} for 3s averaging over forty accumulations.

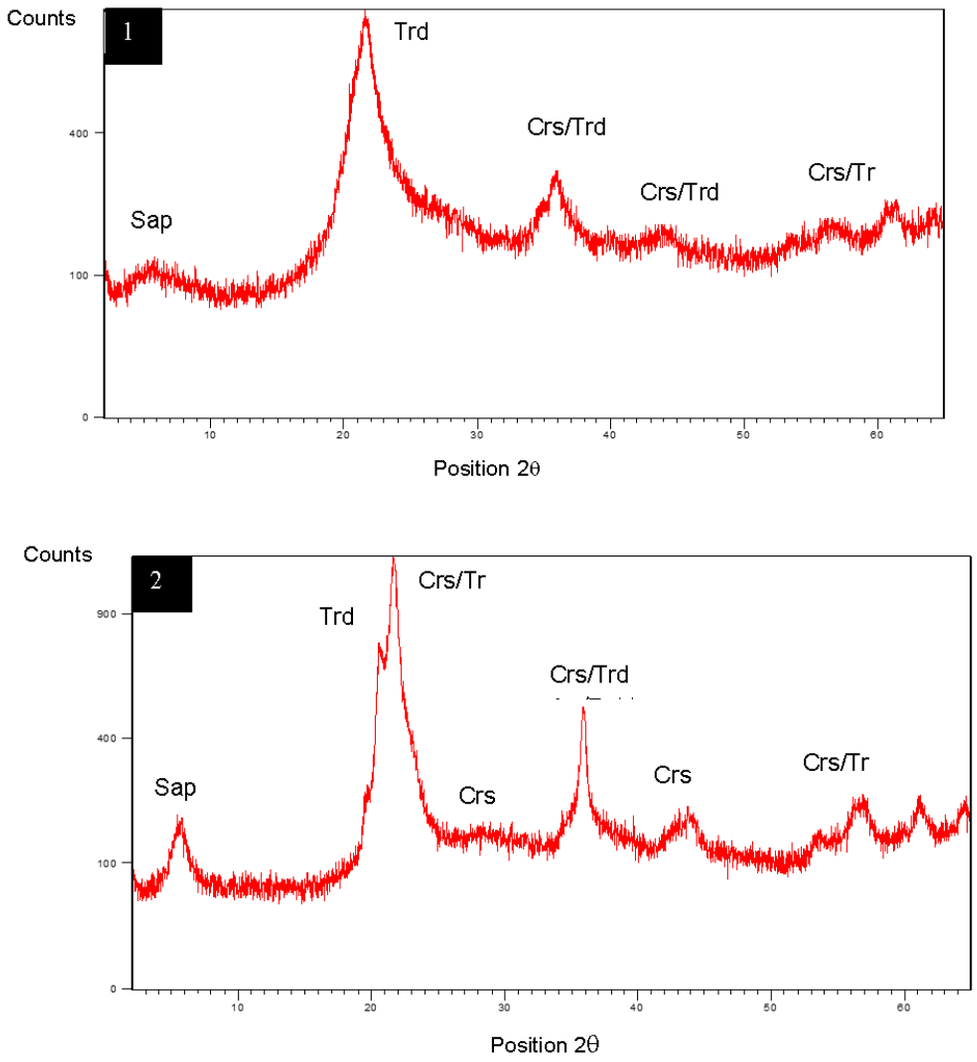

Figure 3. XRPD patterns of the raw samples 1, 2.

Laser - ablation - inductively - coupled plasma - mass spectrometry (LA-ICP-MS) analyses were performed with a double-focusing sector-field ICP-SFMS model Element I, Thermo-Finnigan Mat at IGG-CNR of Pavia, Italy. Fragments of rough and untreated opal were mounted with epoxy on a petrographic carrier glass, and polished with diamond pastes to obtain a mirror finish. Quantification was performed using SiO_2 (stoichiometric value) as internal standard and NIST SRM 610 synthetic glass as external standard. Sample ablation was carried out with 266 nm laser wavelength, with 50 μm nominal beam diameter. Helium was used as carrier gas and mixed with Ar downstream of the ablation cell. Precision and accuracy were estimated by the analysis of a BCR-2 standard and resulted better than 5 and 10%, respectively, for concentrations at ppm level. Detection limits for each element can be found in Miller et al. (2012).

RESULTS

Gemological properties

The gemological properties are reported in Table 1. The gems show a pleasant color with a chromatic variability ranging from green with light yellow shades (styG, samples a and b) to green-yellow (samples c, d, e, f, g). All samples can be considered as common opals without iridescence or play of color.

The specific gravity varies from 2.03 (sample f) to 2.07 (sample b) while refraction indices from 1.435 (sample e) to 1.460 (sample a); these values are in the ranges reported in literature for common opals (Brajkovic et al., 2007; Caucia et al., 2008, 2009, 2012 a,b; 2013 a,b, 2015, 2016, 2019; O'Donaghue, 2006; Simoni et al., 2010).

The samples are inert to both longwave and shortwave UV, the diaphaneity is opaque with a waxy luster. Microscopic observations on gems were carried out with a 32× magnification; the most relevant observed features are the following:

Samples a and b: very porous structure with cavities partially filled with clay minerals; small brown and blackish dendritic spots are also observed; sample c: non-homogeneous color with translucent and lighter opaque areas, presence of black spots; samples d, e and f: presence of black lamellae, veins and fractures; sample g: few dark-colored inclusions.

Table 1. Gemological properties of the investigated samples (gravity, refraction index and color).
*: values measured with distance method; **: values detected with "GIA gemstone color description system.

Sample	Gravity (g/cm^3)	R.I.*	Hue Tone Saturation**
a	2.03	1.460	styG6 3
b	2.07	1.445	styG7 3
c	2.05	1.440	GY6 4
d	2.05	1.439	GY5 4
e	2.05	1.435	GY6 3
f	2.03	1.438	GY6 4
g	2.04	1.440	GY7 4

X-ray powder diffraction (XRPD)

On the base of XRPD data, opals can be divided in three different typologies: amorphous opal (A) essentially made of low temperature amorphous hydrous silica phase; CT opals with disordered stacking sequence of cristobalite and tridymite, C opals mostly constituted of more ordered cristobalite with minor tridymite stacking (Jones and Segnit, 1971; Flörke et al., 1991; Graetsch and Flörke, 1991; Graetsch et al., 1994; Graetsch 1994; Elzeaet al., 1994; Elzea and Rice, 1996; Fritsch et al., 2004; Ghisoli et al., 2010).

Two XRPD patterns of investigated opals are shown in Figure 3 while the results are presented in Table 2. The opals from Anosy belong to the CT type and the Crs/Trd ratios vary from 17/83 to 0/100. Tridymite is more abundant than cristobalite, and samples 3 and 4 are completely made up of tridymite with traces of quartz. In all samples we also observe the presence of a peak at around 14 Å that can be attributed to saponite.

Table 2. "d" values of the characteristic peaks and corresponding C/T ratios of the investigated opals, evaluated through XRPD analyses.

Sample	d (Å)	Crs/Trd (%)
1	4.127	0/100
2	4.098	17/83
3	4.110	0/100
4	4.103	10/90

Trace element geochemistry by LA-ICP-MS

In all the analyzed samples (Table 3), the most abundant elements are Fe with contents between 2.1 and 6.2%, followed by Mg between 1549 and 4886 ppm and Ca between 1122 and 4266 ppm. Other elements present in significant amounts are Ba (110-386 ppm), Al (74-694 ppm), V (26-63 ppm), Na (48-177 ppm), Cu (18-50 ppm), Mn (8-29 ppm), Zn (9-42 ppm), Sr (6-22 ppm), K (20-297 ppm). Finally, some elements have been detected in small

Table 3. Trace element contents obtained through LA-ICP-MS analyses. The elements are reported in ppm with the exception of Fe that, being very abundant, is reported in wt%. The elements that resulted below the detection limits are not reported; detection limits are reported in Miller et al., 2012.

samples	Fe (%)	Mg	Ca	Al	Ba	V	Na	Cu	Zn	Mn	Sr	K	Cr	Ni	Sc	U	Li	Ti
2.1	2.9	2159	1355	336	126	40	44	31	23	15	8	35	8	2.5	3	1	1.5	10
2.2	3.6	2666	2406	124	220	51	75	38	28	17	15	53	3	4.3	2.5	1.7	0.5	1.7
2.3	2.9	2165	2159	83	160	45	77	28	22	14	11	30	5	4.7	2.6	2	8	5
2.4	3.4	2326	2196	102	178	46	80	32	22	19	13	50	2.4	3.5	3	1.8	1	3.1
2.5	3.5	2527	2457	102	221	49	55	34	23	17	14	20	2.5	3.8	3.8	2	1	3
2.6	2.3	1669	1441	77	119	36	52	24	14	11	9	52	6.7	1.5	2.7	1.5	1	8
2.7	2.1	1549	1306	74	110	30	53	24.4	9	10	6	44	6	1.6	1.5	2.7	2.2	7
2.8	4.9	3697	3471	216	303	63	74	49	41	23	22	58	2.4	5.8	2.9	1.5	1.5	2
3.1	3.8	2511	2481	341	222	52	48	34	20	13	13	54	3.8	3.5	2.5	1.3	1.3	4
3.2	3.7	2674	2945	323	200	53	56	41	23	12	14	88	6	4.2	2.1	1.6	2	6.3
3.3	2.7	2276	2086	498	122	32	69	22	15	12	10	52	4	3.2	2.4	1	2.3	2.2
3.4	2.6	2249	1689	410	148	33	61	25	13	11	9	64	4.2	5	2.8	1	1.4	5.3
3.5	3.9	4116	3007	627	208	34	177	35	20	17	17	297	9	6	2.8	1.2	1.1	2.4
3.6	3.9	3777	3420	694	280	39	105	27	23	17	20	168	6	2	3	1	2	15
3.7	2.3	1871	2253	298	121	26	61	25	13	8	9	50	6.3	2	3.2	1.3	1.3	6.4
3.8	4.4	3530	2940	485	204	47	75	33	24	20	15	49	3.3	6	2	1.3	4	2.8
4.1	4.3	3248	2747	130	269	41	78	34.5	25	20	16	35	6.3	2.7	2.4	1.3	2	4.5
4.2	6.2	4886	4266	226	386	60	133	50	35	29	22	135	5	6	3	1	1	6
4.3	2.7	2295	1122	96	195	27	75	18	11.5	16	11	141	16.7	5	3.5	3	5.5	19
4.4	4.9	4115	3497	256	326	46	108	46	42	24	18	107	2.8	6	2.8	1.3	1	2.7

quantities: Cr (3-17 ppm), Ni (2-6 ppm), Li (1-8 ppm), Sc (2-4 ppm), Ti (2-19 ppm) and U (1-3 ppm).

The most relevant positive correlations are Fe-Mg (Figure 4a), Ca-Fe (Figure 4b), Ca-Mg (Figure 4c), Ba-Fe (Figure 4d), Ba-Mg (Figure 4e), Ba-Ca (Figure 4f), Sr-Ba (Figure 4g), Ba-Mn (Figure 4h).

In the magmatic geological setting, opals are generally formed by precipitation from hydrothermal fluids rich in silica. If the system is open, these fluids can also alter the surrounding rocks causing an increasing of several trace elements in the opals.

Since the type of source rocks of the Anosy region is very variable it is difficult to accurately establish the origin of the chemical elements in the opals but it is possible to advance the following hypothesis: the abundances of Fe are positively correlated with Mg as these two elements are commonly associated in mafic minerals such as olivine, pyroxenes and mica (especially biotite), while the correlations between Ca with Fe and Mg indicate more clearly a provenance from pyroxenes or amphiboles. Correlations of Ba with Ca, Mg, Fe, Sr and Mn indicate a common origin from different types of micas and feldspars (Edgar, 1992; Shaw and Penczak, 1996; Icenhower and London, 1996).

Although the correlations are not very good, we observe that the samples with highest K also show the highest Na and Ca contents; this would indicate a common origin from feldspars and mica. Finally, Mg, Al, Na and Fe are also associated with the presence of smectite/saponite.

Aluminium contents are high but show no relevant correlations with other elements. Al is frequently the most abundant impurity in opals and locally replaces silicon; the charge imbalance is compensated by the entry of monovalent or divalent cations such as Na^{+}, K^{+}, Ba^{2+}, Mg^{2+}, Ca^{2+} (Bartoli et al., 1990; Gaillou et al., 2008 a,b; Caucia et al., 2016, 2019).

SEM investigation

SEM observations of microstructures in opals allow us to better understand their genesis. According to the literature amorphous opals consist largely of silica spheres of almost uniform size, with a diameter between 150-300 nm while C and CT opals are composed of spherules of variable size and random arrangement. Amorphous opals

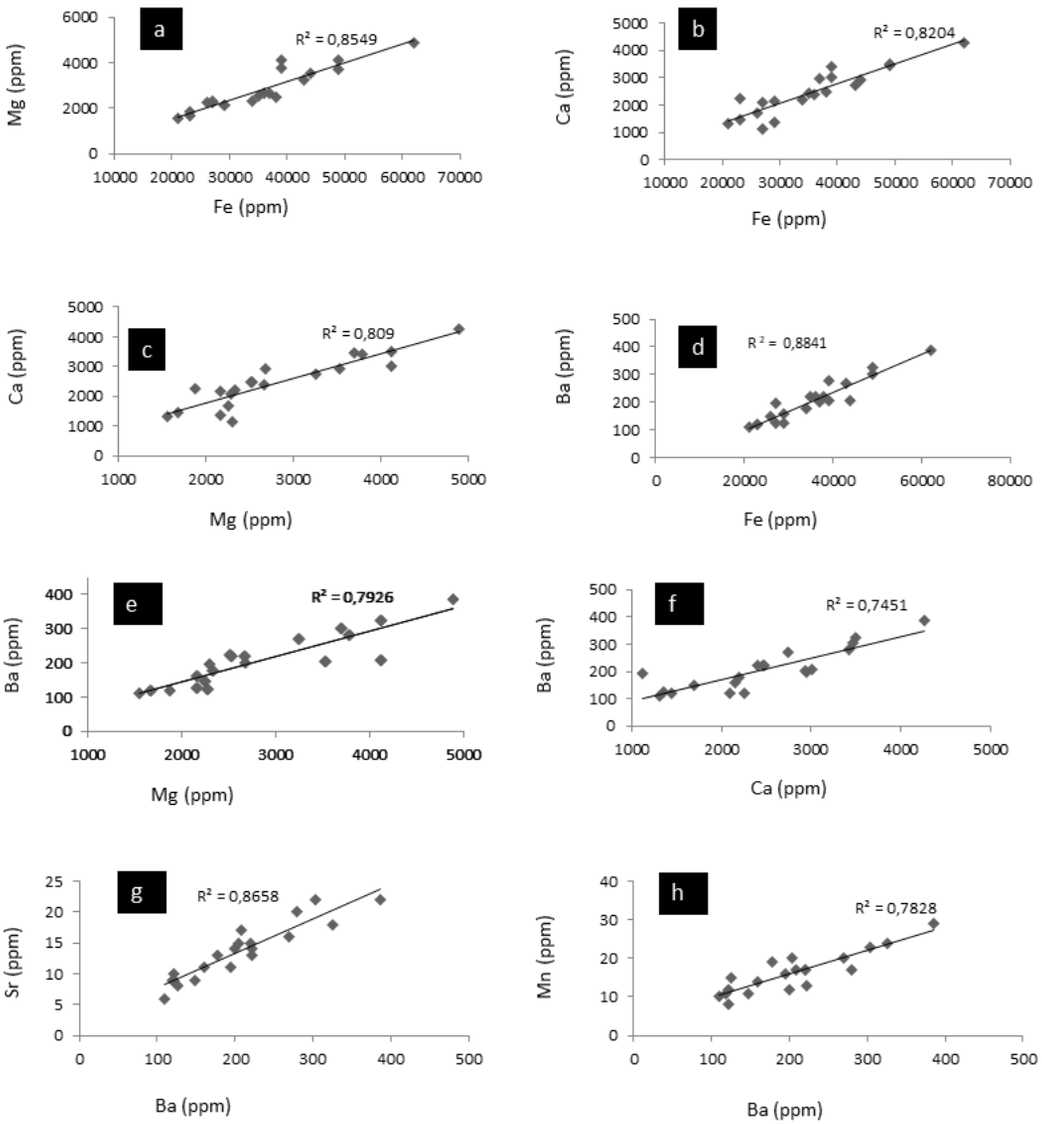

Figure 4. (a-h) Plots of the correlations between Fe-Mg, Fe-Ca, Mg-Ca, Fe-Ba, Mg-Ba, Ca-Ba, Ba,Sr, Ba-Mn contents in the samples 2, 3, 4.

are generally of sedimentary, tectonic or hydrothermal origin (low temperature), while C and CT opals are mainly magmatic (Sanders, 1964; Jones et al., 1964; Rondeau et al., 2004; Gaillou et al., 2008a and references therein; Ghisoli et al., 2010).

Most of C and CT opals are formed through deposition processes from hydrothermal fluids in volcanic areas, during long periods of inactivity. In some cases C and CT opals also derive from the diagenetic transformation of previous amorphous opals (Koivula et al., 1983; Lynne and Campbell, 2004).

In the common C and CT opals, four different types of microstructure are described (Greer, 1969; Sanders and Murray, 1978; Murray and Sanders, 1980; Graetsch, 1994; Rossman, 1994; Fritsch et al., 1999; Gaillou et al., 2008b and references therein; Caucia et al., 2013, 2015; 2019).

1) massive microtexture composed of siliceous cement and, at times, amorphous silica nano-granules that appear too small to be observed even by SEM;

2) microtexture composed of randomly arranged microspheres, or nano-granules, of amorphous silica with dimensions of about 10-40 nm;

3) microtexture composed of lepispheres, in which the nano-granules are organized in agglomerates of different morphology and various sizes (from 200 nm to 20 μm).

4) fibrous microtexture, due to the presence of

phyllosilicates bound to amorphous silica spheres. These fibers appear as single or associated in bundles or strips.

Figure 5 shows the microtextures of opal samples investigated in this work (opals 2, 3 and 4). Sample 2 (Figure 5 a,b) shows two different microtextures: in the microphoto b we observe a very dense and finer microstructure, alternating with zones with agglomerated microgranules (250 nm). In the Figure 5 a we can observe the coarse portion made up of lamellae, inside fractures and cavities; the microspheres are approximately 0.1 µm.

Sample 3 shows dense and homogeneous areas of stacked nano-spheres (Figure 5c) alternating with lepispheric "cauliflower" type microtextures with variable particle size (Figure 5d).

In the sample 4 we observe a dense microtexture formed by amorphous silica micro-granules with pseudo-parallel

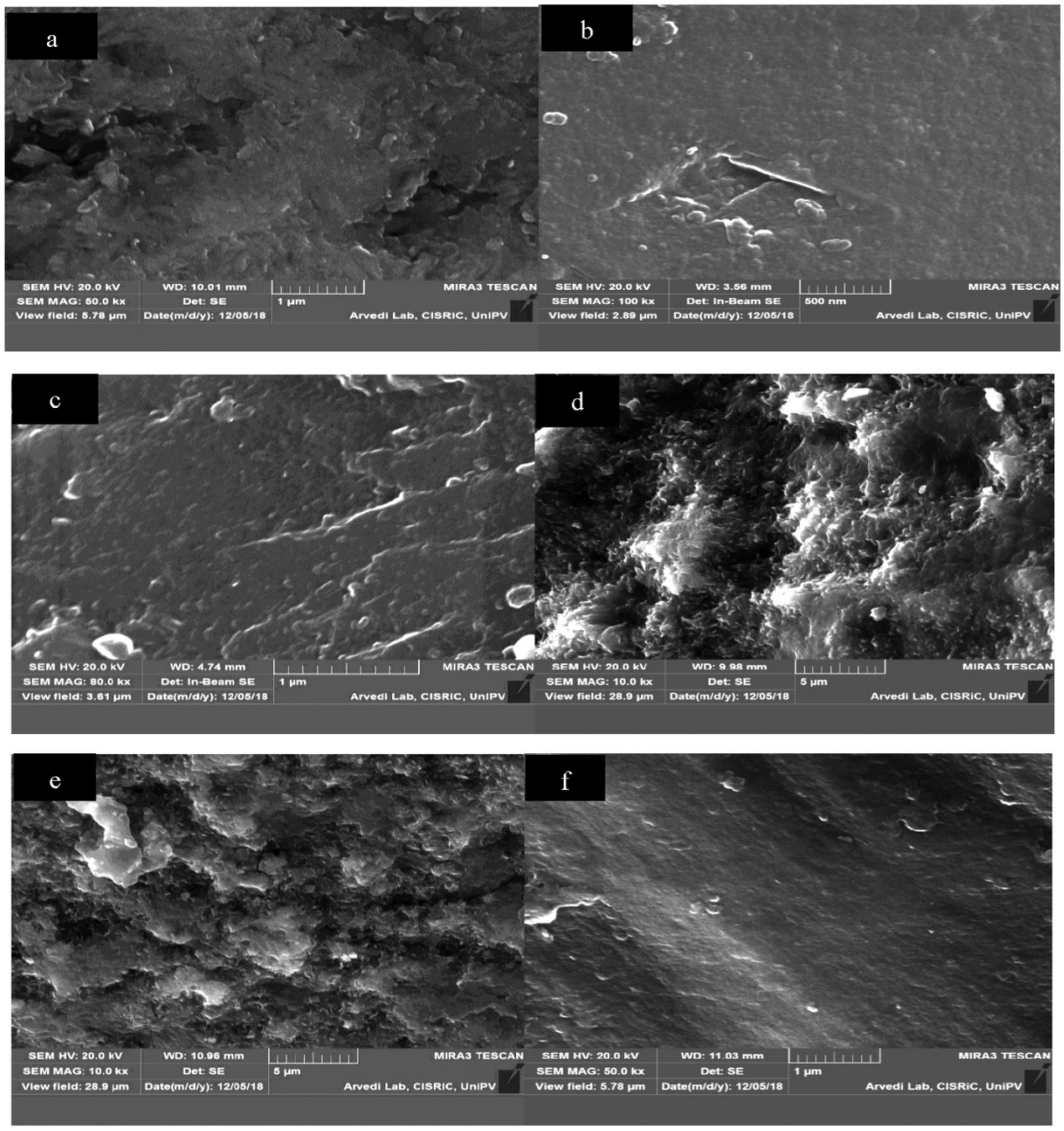

Figure 5. SEM microphotos of the samples 2 (photos a and b), 3 (photos c and d), 4 (photos e and f).

growth lines and hints of channels (Figure 5e). Figure 5f shows a spongy microtexture with globular aggregates of different sizes formed by laminae and columns about 1 µm long.

Micro-Raman Spectroscopy

Micro-Raman spectroscopy is a non-destructive method that allows probing to short-range structural order and water content and can provide important information for the classification and characterization of the opals. This technique allows to further discriminate two phases of opals showing very similar XRPD patterns and can therefore implement the information obtained through the previous technique. In addition unlike XRPD, Raman Spectroscopy allows to perform analyzes on the unground sample and on specific parts of a gem, choosing for example those with different colors. Raman spectra of tridymite and cristobalite respectively show strong bands between 300-405 $cm^{-1}$and 231-418 cm^{-1}. When the diagnostic peaks of cristobalite and tridymite show similar intensity and width, the structure is very close to that of CT opal, consisting of the alternation of nano-tridymite and cristobalite domains. Amorphous opal is instead characterized by a broad band with a maximum at 430 cm^{-1} (Smallwood et al., 1997; Ilieva et al., 2007; Ostrooumov, 2007; Wilson, 2014; Sodo et al., 2016; Caucia et al., 2019).

In Figure 6 we report the micro-Raman spectra of the opal gems e and f in the wave ranges between 50-1200 cm^{-1}(where opals show the strongest Raman signal, a) and between 3000-3800 cm^{-1}(where O-H and H_2O bonds are present, b). The spectra of the two samples are very similar.

The signals in the range 200-600 cm^{-1} are typical of the O-Si-O and Si-O-Si bending vibrations of silicate structures: in our samples these bands are not very wide and this indicates that the structure is significantly crystalline (i.e., not completely amorphous). This evidence is also confirmed by the band at about 485-493 cm^{-1}, which is characteristic of amorphous silica and appears very weak and wide (Ostrooumov et al., 1999; Ilieva and Mihailova, 2002; Caucia et al., 2019).

In the samples investigated in this work the maximum is centered at 350 cm-1, indicating the prevalence of tridymite structural units with respect to cristobalite; for this reason the sample can be considered as a CT-T opal (according to the current nomenclature).

The band at 780 cm^{-1} can be attributed to the symmetrical stretching vibration Si-O-Si while the weak band at about 1065 cm^{-1} to the Si-O anti-symmetrical stretching vibration (Ilieva et al., 2007). The bands in the range 3000-3600 cm^{-1} are generated by the O-H bond stretching modes of the hydrous species incorporated in the silicate matrix; these bands are well resolved in the spectrum of the investigated opal. Lastly the presence of clay mineral (mixed layer saponite-nontronite) is confirmed by the modest signals at 175 cm^{-1} and at 890 and 1030 cm^{-1} (Frost and Kloprogge, 2000). In conclusion the results from Micro-Raman spectroscopy support XRPD analysis.

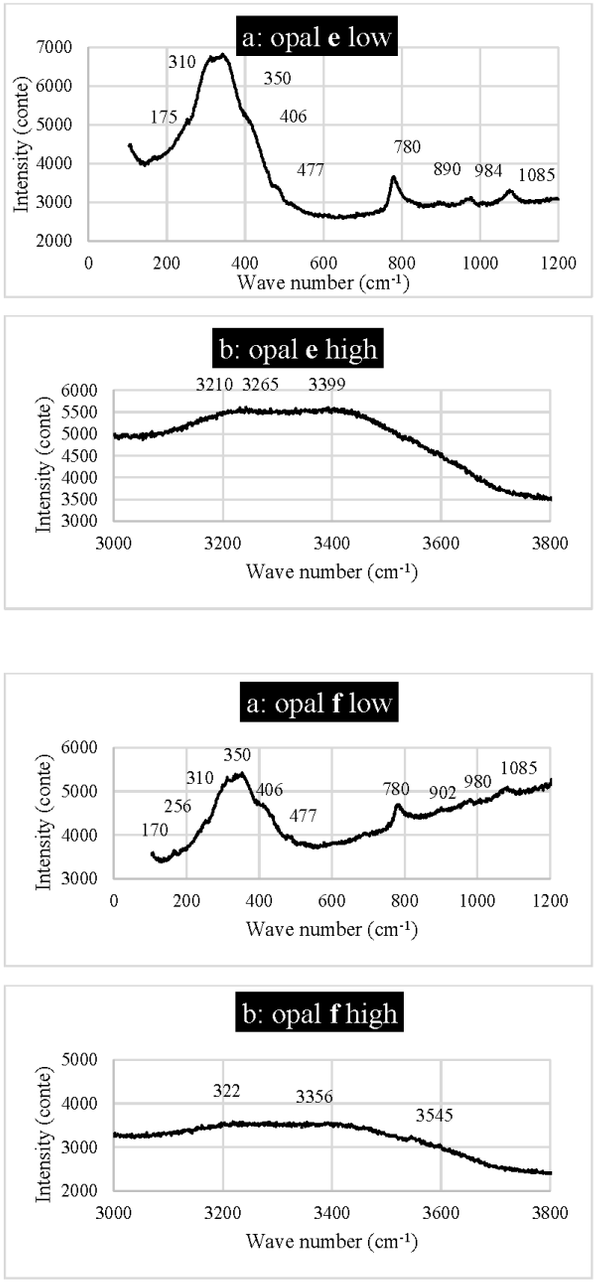

Figure 6. Raman spectra of the sample e: a) wave number between 200 and 1200 cm^{-1}, b) wave number between 3000 and 3800 cm^{-1}; Raman spectra of the sample f: a) wave number between 200 and 1200 cm^{-1}, b) wave number between 3000 and 3800 cm^{-1}.

DISCUSSION

The geochemical and mineralogical investigation in opals allows to understand the correlations between the color of the gemstone and the inclusions of other minerals (oxides, sulphides, clay minerals) and the abundances of chromophore elements (Sanders, 1964; Mc Orist and Smallwood, 1997; Fritsch et al., 1999, 2004; Gaillou et al., 2008a; Simoni et al,. 2010; Caucia et al., 2009, 2012a, 2013 a,b, 2015, 2016, 2019; Koivula and Fryer, 1984; Koivula and Kammering, 1991). The elemental abundances indicate that the main chromophores which attribute the green color to our opals are Fe and to a lesser extent V and Cu. Important chromophores for the green color such as Ni and Cr are present in very small quantities and therefore do not contribute to the color. Microscopy observation showed the gems are characterized by an inhomogeneous color, due to the presence of cavities partly empty and partly filled with clayey materials, black lamellae and brown or blackish spots. The presence of saponite detected by XRPD and Micro-Raman analyses gives to the samples a characteristic waxy-greasy luster described as "fat". The most significant geochemical feature of our samples is the high contents of Ba (110-386 ppm) as this element is rarely reported in the CT opals around the world.

Ba is present in sedimentary opals from Australia and Brazil (Gaillou et al., 2008a) and has been found, albeit in lower amounts, in the fire opals from Bemia in Madagascar (Simoni et al., 2010). Due to its rarity in opals around the world, Ba can therefore be considered a geochemical marker of Anosy opals. The positive correlations of Ba with Ca, Mg, Fe, Sr and Mn indicate a common origin from different types of micas and feldspars.

Raman and XRPD analyses indicated the investigated samples are characterised by good compositional homogeneity, since tridymite is prevalent compared to cristobalite. Similarly, the SEM observations also showed that the microstructures of the samples are quite similar with the presence of lepispheres, and correspond to those observed in magmatic opals. All these evidences suggest that opals formed under similar genetic conditions, with a slow or moderate growth rate (Gaillou et al., 2008b; Caucia et al., 2013b).

CONCLUSIONS

Most common opals reported in literature show a green color, determined by chromophore elements such as Fe, V, Cr, Ni and Cu. The opals of Anosy show a pleasant green color, although not very homogeneous, and the main cromophore is represented by Fe.

Common Anosy opals would certainly have good commercial value as semi-precious materials, although lower than that of fire opals from Bemia in Madagascar and other regions of the world as well. Our research conducted so far would indicate that the most precious common green opals contain little Fe and the chromophore elements are preferably represented by Ni and Cu. Ni is in fact the most important chromophore in opals from Haneti in Tanzania and Eastern Rhodopes in Bulgaria (Caucia et al., 2016; Caucia et al., 2019) while Cu is the determining cromophore in the opals from Acari Mine in Peru (Caucia et al., 2015). Ni and Cu would give the opals a lower tone in the GIA scale and a better saturation (i.e. purity of the green color) and the gems are therefore more marketable.

Furthermore, Fe as a chromophore element in opals produces commercially more appreciated gems when is present in trivalent state. In fact, the opals from the neighboring region of Bemia are rich in Fe^{3+} which gives them a color varying from creamy to reddish orange and can be commercially classified as fire opals (Simoni et al., 2010). For these characteristics, Bemia opals have a market value certainly higher than those of Anosy.

ACKNOWLEDGEMENTS

The authors are grateful to Antonio Langone for the assistance with LAM-ICP-MS analysis and to Massimo Boiocchi for the assistance of the realization of the graphs.

REFERENCES

Ashwal L.D. and Tucker R.D., 1999. Geology of Madagascar: a brief outline. Gondwana Research 2, 335-339.

Bank H., Henn U., Milisenda C.C., 1997. Green opal from Turkey (in: Gemmological News). Zeitschrift der Deutschen Gemmologischen Gesellschaftl 46, 2-3.

Bartoli F., Bittencourt Rosa D., Doirisse M., Meyer R., Philippy R., Samama J.C., 1990. Role of aluminium in the structure of Brazilian opals. European Journal of Mineralogy 2, 611-619.

Brajkovic A., Rolandi V., Vignola P., Grizzetti R., 2007. Blue and pink opals from Acari, Peru- their optical, structural and spectroscopic features. Australian Gemmologist 23, 3-15.

Brandt S., Raith M.M., Schenk V., Sengupta P., Srikantappa C., Gerdes A., 2014. Crustal evolution of the Southern Granulite Terrane, south India: New geochronological and geochemical data for felsic orthogneisses and granites. Precambrian Research 246, 91-122.

Caucia F., Ghisoli C., Adamo I., Bocchio R., 2008. Opals-C, opals-CT and opals-T from Acari, Peru: X-ray powder diffraction analysis and IR spectroscopy investigation of new samples showing two different typologies of luster. Australian Gemmologist 23, 266-271.

Caucia F., Ghisoli C., Adamo I., 2009. A study on the characteristics of some C- and CT-opals from Brasil. Neues Jahrbuch Mineralogie Abhandlungen 185, 288-296.

Caucia F., Ghisoli C., Marinoni L., Bordoni V., 2012a. Opal, a beautiful gem between myth and reality. Neues Jahrbuch Mineralogie Abhandlungen 190, 1-9.

Caucia F., Marinoni L., Bordoni V., Ghisoli C., Adamo I., 2012b. Physical and chemical properties of some italian opals. Periodico di Mineralogia 81, 93-106.

Caucia F., Marinoni L., Leone A., Adamo I., 2013a. Investigation on the gemological, physical and compositional properties of some opals of Slovakia ("Hungarian" opals). Periodico di Mineralogia 82, 251-261.

Caucia F., Marinoni L., Leone A., 2013b. Physical, geochemical and gemological properties of opals from Faroe Islands. Neues Jahrbuch Mineralogie, Abhandlungen (Journal of Mineralogy and Geochemistry) 191, 33-43.

Caucia F., Marinoni L., Leone A., Ghisoli C., 2015. New physical, geochemical and gemological data of opals from Acari Mine (Arequipa Department, Peru). Neues Jahrbuch Mineralogie Abhandlungen (Journal of Mineralogy and Geochemistry) 192, 73-84.

Caucia F., Marinoni L., Ghisoli C., Leone A., 2016. Gemological, physical and chemical properties of prase opals from Hanety Hill (Tanzania). Periodico di Mineralogia 85, 41-50

Caucia F., Marinoni L., Bruni G., 2019. Investigation on the gemological, physical and compositional properties on some green opals from Eastern Rhodopes. Rendiconti Accademia Lincei Scienze Fisiche e Naturali.

Eckert A.W., 1998. The world of Opals. New York and Chichester (John Wiley & Sons, Inc.), p. 448.

Edgar A.D., 1992. Barium-rich phlogopite and biotite from some Quaternary alkali mafic lavas, West Eifel, Germany. European Journal of Mineralogy4, 321-330.

Elzea J.M., Odom I.E., Miles W.J., 1994. Distinguishing well ordered opal-CT and opal-C from high temperature cristobalite by X-ray diffraction. Analytical Chimica Acta 286, 107-116.

Elzea J.M. and Rice S.B., 1996. TEM and X-Ray Diffraction evidence for cristobalite and tridymite stackings sequences in opals. Clays Clay Minerals 44, 492-500.

Esenli F., Kumbasar I., Eren R.E., Uz B., 2001. Characteristics of opals from Simav, Turkey. Neues Jahrbuch Mineralogie, Monathshefte 3, 97-113.

Flörke O.W., Graetsch H., Martin B., Röller K., Wirth R., 1991. Nomenclature of micro- and non-crystalline silica minerals, based on structure and microstructure. Neues Jarhbuch Mineralogie Abhandlungen 163, 19-42.

Fritsch E., Rondeau B., Ostrooumov M., Lasnier B., Marie A.M., Barrault A., Wery J., Connoué J., Lefrant S., 1999. Découvertes recente sur l'opale. Revue de Gemmologie a.f.g. 138/139, 34-40.

Fritsch E., Gaillou E., Ostrooumov M., Rondeau B., Devouard B., Barreau A., 2004. Relationship between nanostructure and optical absorption in fibrous pink opals from Mexico and Peru. European Journal of Mineralogy 16, 743-752

Frost R.L. and Kloprogge J.T., 2000. Raman spectroscopy of nacrite single crystals at 298 and 77K. Spectrochimica Acta A 56, 931-939.

Gaillou E., Delaunay A., Rondeau B., Bouhnik Le Coz M., Fritsch E., Cornen G., Monnier C., 2008a. The geochemistry of gem opals as an evidence of their origin. Ore Geology Reviews 34, 127-133.

Gaillou E., Fritsch E., Auguilar-Reyes B., Rondeau B., Post J., Barreau A., Ostrooumov M., 2008b. Common gem opal: An investigation of micro- to nano-structure. American Mineralogist 93, 1865-1873.

Ghisoli C., 2008. Opali-caratterizzazione, definizione nomenclatura e nuova proposta di classificazione delle varietà, alla luce della scoperta di nuovo materiale peruviano. PHD Thesis, University of Pavia.

Ghisoli C., Caucia F., Marinoni L., 2010. XRPD patterns of opals: a brief revue and new results from recent studies. Powder Diffraction 25, 274-282.

Graetsch H. and Flörke O.W., 1991. X-Ray powder diffraction patterns and phase relationship of tridymite modifications. Zeitschrift Kristallographie 195, 31-48.

Graetsch H., 1994. Structural characteristics of opaline and mirocrystalline silica minerals. (In: Heaney P.J., Prewitt C.T., Gibbs G.V., Eds.) Silica, physical behavior, geochemistry and materials applications), Reviews in Mineralogy and Geochemistry 29, 209-232.

Graetsch H., Gies H., Topalovic I., 1994. NMR, XRD and IR study on microcrystalline opals. Physics and Chemistry of Minerals 21, 166-175.

Greer R.T., 1969. Submicron structure of "amorphous" opal. Nature 224,1199-1200.

Hatipoglu M. and Yardimci Y., 2014. Optical and cathodoluminescence investigation of the green microcrystalline (chrisoprase) quartz. Journal Luminescence Applications, 87-104.

Hatipoglu M., Kibici Y., Yanik G., Ozkul C., Demirbilek M., Yardimci Y., 2015. Nano-structure of the tridymite stacking sequences in the common purple opal from the Gevrekseydi deposit, Seyitömer-Kütahya, Turkey. Oriental Journal Chemistry 31, 35-49.

Icenhower J.P. and London D., 1996. Experimental partitioning of Rb, Cs, Sr and Ba between alkali feldspar and peraluminous melt. American Mineralogist 81, 719-734.

Ilieva A. and Mihailova B., 2002. Structural state of opal in opal siliceous rocks, Eastern Rhodopes. Comptes Réndus Académie Bulgare des Sciences 55, 65-70.

Ilieva A., Mihailova B., Tsintov Z., Petrov O., 2007. Structural state of microcrystalline opals: a Raman spectroscopic study. American Mineralogist 92, 1325-333.

JCPDS, 1986. Mineral Powder Diffraction File. Data Book. The International Centre for Diffraction Data, USA.

Jones J.B., Sanders J.V., Segnit E.R., 1964. Structure of opal. Nature 204, 990-991.

Jones J.B. and Segnit E.R., 1971. The nature of opal. I. Nomenclature and constituent phases. Journal of Geological Society of Australia 18, 57-68.

Koivula J.I., Fryer C.W., Keller P.C., 1983. Opal from Querétaro,

Mexico: occurrence and inclusions. Gems & Gemology 19, 87-96.

Koivula J.I. and Fryer C.W., 1984. Green opal from East Africa. Gems& Gemology 20, 226-227.

Koivula J.I. and Kammerling R.C., 1991. More of Peruvian opal (In: Gem News) Gems & Gemology 27, 259-260.

Lacroix A., 1922. Mineralogie de Madagascar. Vol. 1, Augustin Challamel éditeur, Paris, France, 269-273.

Lynne B.Y. and Campbell K.A., 2004. Morphologic and mineralogic transitions from opal-A to opal-CT in low temperature siliceous sinter diagenesis, Tapuo volcanic zone, New Zealand. Journal of Sedimentary Research 74, 561-579.

Mc Orist G.D. and Smallwood A., 1997. Trace elements in precious and common opals using neutron activation analysis. Journal of Radioanalytical and Nuclear Chemistry 223, 9-15.

Miller C., Zanetti A., Thöni M., Konzett J., Klötzli U., 2012. Mafic and silica-rich glasses in mantle xenoliths from Wau-en-Namus, Lybia: Textural and geochemical evidence for peridotite-melt reactions. Lithos 128,11-26.

Moine B. and Nedelec A., 2014. Geology and metallogeny of the Precambrian basement of Madagascar. Journal African Earth Sciences 94, 1-8.

Moore D.M. and Reynolds-Jr R.C., 1997. X-ray diffraction and the identification and analysis of clay minerals. 2nd Edition. Oxford University Press, New York, New York State.

Neymark L.A., Amelin Y.V., Paces J.B., 2000. ^{206}Pb-^{230}Th-^{234}U-^{238}Pb and ^{207}Pb-^{235}U geochronology of Quaternary opal, Yucca Mountain, Nevada. Geochimica Cosmochimica Acta 64, 2913-2928.

O'Donoghue M., 2006. Gems, 6th ed. Butterworth-Heinemann, Oxford, United Kingdom.

Ostrooumov M., Fritsch E., Lasnier B., Lefrant S., 1999. Spectres Raman des opales: aspect diagnostique et aide à la classification. European Journal of Mineralogy 11, 899-908.

Ostrooumov M., 2007. A Raman, infrared and XRD analysis of the instability in volcanic opals from Mexico. Spectrochimica Acta A 68, 1070-1076.

Rondeau B., Fritsch E., Guiraud M., Renac C., 2004. Opals from Slovakia ("Hungarian" opals): a re-assessment of the conditions of formation. European Journal of Mineralogy 16, 789-799.

Rossman G.R., 1994. Colored varieties of silica minerals: Opal (in: Heaney PJ, Prewitt CT Gibbs GV (Eds.), Silica, physical behavior, geochemistry and materials applications) Reviews in Mineralogy 29, 460-462.

Sanders J.V., 1964. Colour of precious opal. Nature 275, 201-203.

Sanders J.V. and Murray M.S., 1978. Ordered arrangement of spheres of two different sizes in opal. Nature 275, 201-203.

Shaw C.S. and Penczak R., 1996. Barium- and titanium-rich biotite and phlogopite from the Western and Eastern Gabbro, Coldwell alkaline complex, Northwestern Ontario. Canadian Mineralogist 34, 967-975.

Simoni M., Caucia F., Adamo I., Galinetto P., 2010. New occurrence of fire opal from Bemia, Madagascar. Gems & Gemology 46, 114-121.

Smallwood A.G., Thomas P.S., Ray A.S., 1997. Characterization of sedimentary opals by Fourier transform Raman spectroscopy. Spectrochimica Acta Part A 53, 2341-2345.

Sodo A., Casanova Municchia A., Barucca S., Bellatreccia F., Della Ventura G., Butini F., Ricci M.A., 2016. Raman, FT-IR and XRD investigation of natural opals. Journal Raman Spectroscopy Published online in Wiley Online Library, John Wiley & Sons, p. 8.

Wilson M.J., 2014. The structure of opal-CT revisited. Journal Non-Crystal Solids 405, 68-75.